





# Role of magnetic resonance imaging in the differentiation of mucinous ovarian carcinoma and mucinous borderline ovarian tumors

Ebru Hasbay<sup>1\*</sup> , Gökşen Görgülü<sup>2</sup> , Muzaffer Sancı<sup>2</sup> , Birsen Gizem Özamrak<sup>3</sup> 

## SUMMARY

**OBJECTIVE:** This study was carried out to investigate the differentiation of mucinous borderline ovarian tumor from mucinous ovarian carcinoma using magnetic resonance imaging.

**METHODS:** We evaluated 77 women patients who underwent abdominal magnetic resonance imaging due to pelvic mass. magnetic resonance imaging was reviewed by an experienced radiologist. A total of 70 women patients were included in the study. The magnetic resonance imaging features were retrospectively evaluated and compared between the two pathologies.

**RESULTS:** There was no difference between the two groups in terms of maximum tumor size. Age at diagnosis was  $56.29 \pm 11.92$  in the mucinous ovarian carcinoma group and  $44.74 \pm 13.60$  in the mucinous borderline ovarian tumor group ( $p < 0.05$ ). A significant difference was found between the two groups, and it was observed that mucinous borderline ovarian tumors appeared in the younger age group compared to mucinous ovarian carcinomas. Presence of ascites, peritoneal dissemination, lymphadenopathy, and mural nodules was found significantly more frequently in mucinous ovarian carcinomas than in mucinous borderline ovarian tumors. Honeycomb appearance was found more frequently in mucinous borderline ovarian tumor patients than in mucinous ovarian carcinoma patients.

**CONCLUSION:** magnetic resonance imaging findings of these two pathologies overlapped considerably. Compared with mucinous borderline ovarian tumors, mucinous ovarian carcinomas frequently had mural nodules larger than 5 mm, larger tumor size, peritoneal dissemination, and abnormal ascites.

**KEYWORDS:** Magnetic resonance imaging. Mucinous carcinoma. Ovary. Epithelial ovarian cancer.

## INTRODUCTION

Mucinous ovarian neoplasms constitute 10–15% of epithelial ovarian neoplasms<sup>1</sup>. mucinous cystadenomas constitute 80% of ovarian mucinous neoplasms, while MBOTs and MOCs constitute about 16–17% and 3–4% of them, respectively<sup>1</sup>. Borderline tumors were first described as semi-malignant mass lesions<sup>2</sup>. They are histopathologically malignant but do not show invasive features, and their clinical course is quiescent<sup>3</sup>. Mucinous neoplasms can appear morphologically as giant multicystic masses. Therefore, magnetic resonance imaging (MRI) findings may be similar between these three subtypes<sup>4</sup>.

Mucinous-derived lesions can show multiloculations. The formation of different signals in T1- and T2-weighted sequences of such loculations is described as “stained glass appearance.”

This finding is accepted as one of the characteristic MRI findings of mucinous neoplasms<sup>5,6</sup>.

According to the generally accepted view, a contrasting solid component or thick septa in a cystic mass in epithelial ovarian tumors is considered significant for malignancy<sup>7-10</sup>. In addition, in previous studies on mucinous neoplasms, honeycomb-shaped loculations, T1 hyperintense, T2 hypointense intracystic signal, thick septa, and a cyst wall thicker than 5 mm were observed significantly more frequently in MBOTs than MOCs<sup>7-10</sup>.

As most of the patients with MBOT are young, fertility-sparing surgery can be considered in this patient group. However, in patients with carcinoma, the main treatment is surgery and adjuvant or neoadjuvant chemotherapy<sup>11</sup>. Therefore, we aimed to describe, compare, and find differences in MRI findings

<sup>1</sup>University of Health Sciences, Tepecik Education and Research Hospital Center, Department of Radiology – Izmir, Turkey.

<sup>2</sup>University of Health Sciences, Tepecik Education and Research Hospital Center, Department of Gynaecologic Oncology – Izmir, Turkey.

<sup>3</sup>University of Health Sciences, Tepecik Education and Research Hospital Center, Department of Pathology – Izmir, Turkey.

\*Corresponding author: ebruhasbay@gmail.com

Conflicts of interest: the authors declare there is no conflicts of interest. Funding: none.

Received on March 25, 2023. Accepted on April 27, 2023.

between MBOT and MOC in our patients to improve the precision of the preoperative diagnosis.

## METHODS

### Patients

In our retrospective study, 45 patients with MBOT and 32 patients with MOC, diagnosed between February 2011 and September 2022, were included after approval from the ethics committee of our hospital. Two patients with MBOT and three patients with MOC were excluded from the study because their MR images could not be accessed. Another two patients with MOC were also excluded because their MR images were of poor technical quality.

### Magnetic resonance imaging technique

MRI examinations were performed with the standard protocol using a 1.5 T MRI system (Siemens Avanto, Siemens Aera, GE Optima360) with a pelvic phased-array coil. The protocol included sagittal, axial, and coronal T2-weighted images without fat saturation, axial T2-weighted fat-saturated images, and axial T1-weighted fat-saturated gradient-echo images before and after intravenous contrast administration (Gadoteric acid, Dotarem®, Guerbet, Paris, 0.1 mmol/kg).

### Image analysis

As MRI findings, among morphological features, tumor diameter, T2 hypointense component, mural nodule (MN), number of septa, thick septa (5 mm), honeycomb appearance, stained glass appearance, presence of ascites, and peritoneal spread were evaluated.

A solid component adhering to the septa or cyst wall was described as a mural nodule, and the evaluation was made with T2 and/or contrast-enhanced images. The number of loculations was evaluated quantitatively as 1–10, 10–20, and 20–30. Septa thickness of 5 mm and above was described as thick septa. The presence of multiple cysts, 5–10 mm in size and located in close proximity to each other, was evaluated as honeycomb appearance. Stained glass appearance was evaluated according to the different signal formations of intraloculation loculations in T1- and T2-weighted sequences. T2 hypointense cyst was considered isointense or slightly hyperintense on T2-weighted sequences when compared to adjacent muscle tissue. While assessing the ascites, the presence of ascites exceeding the level of uterine fundus and/or filling the pelvic cavity was evaluated as a positive finding, and fluid at the Douglas level was counted as

physiological. All findings were reviewed by an experienced abdominal radiologist.

### Statistical analysis

Statistical analyses were performed using SPSS 24.0 (IBM Corp., Armonk, NY, USA) program. Normality tests, skewness-kurtosis values, and histogram graphs were used to determine whether the numerical variables were normally distributed. Student's t-test was used to determine whether numerical variables differed significantly between groups, and the  $\chi^2$  test was used to determine the differences between categorical variables between groups. Variables that differed between the two groups were included in the logistic regression analysis. The variables determining the differences between the groups were investigated with the logistic regression analysis applied with the "Enter" method. A p-value of <0.05 was considered significant in all statistical analyses.

## RESULTS

In our study, 27 patients with MOC and 43 patients with MBOT were included. Age at the time of diagnosis was  $56.29 \pm 11.92$  in the MOC group and  $44.74 \pm 13.60$  in the MBOT group ( $p < 0.05$ ). There was no significant difference between the two groups regarding maximum tumor size. The mean tumor size was  $203.55 \pm 79.66$  mm in the MOC group and  $175.11 \pm 88.93$  in the MBOT group ( $p < 0.180$ ).

Categorical variables are summarized in Table 1. According to these findings, ascites, peritoneal carcinomatosis, lymphadenopathy (LAP), and mural nodules were observed significantly more frequently in MOCs than in MBOTs. In addition, honeycomb appearance was more commonly seen in MBOT patients than in MOC patients. The number of loculi, the presence of the T2 hypointense component, and stained glass appearance were emphasized and studied in previous research. However, in our study, there was no significant difference between the groups regarding those parameters.

The variables that differed between these two groups were included in the logistic regression analysis afterward. We identified the variables that had a direct and independent effect on the determination of the groups. As shown in Table 2, "honeycomb appearance" and "thick septa" have determined the difference between groups independently and directly. Beta value was positive in the presence of honeycomb sign and was negative in the presence of thick septa. This finding was interpreted as the "honeycomb sign" directly predicts the presence of MBOT and is considered to have diagnostic significance, while "thick septa" is found to predict the MOC group directly.

**Table 1.** Comparison of qualitative variables between groups.

Variables	MOC (n=27)	MBOT (n=43)	Statistical analysis*	
	n (%)	n (%)	$\chi^2$	p-value
Abnormal ascites	9 (33.3)	5 (11.6)	4.88	<b>0.027</b>
Peritoneal carcinomatosis	9 (33.3)	0 (0)	16.44	<b>&lt;0.0001</b>
Mural nodule (>5 mm)	17 (63.0)	10 (23.3)	11.03	<b>0.001</b>
Honeycomb sign	10 (37.0)	32 (74.4)	9.65	<b>0.002</b>
Septa (>5 mm)	26 (96.3)	26 (61.9)	10.46	<b>0.001</b>
Stained glass appearance	7 (25.9)	15 (34.9)	0.61	0.432
T2 hypointense cyst	11 (40.7)	12 (27.9)	1.23	0.266
Loculi (10–20)	4 (14.8)	9 (20.9)	0.41	0.522
Loculi (20–30)	1 (3.7)	8 (18.6)	3.28	0.070
Loculi (>30)	22 (81.5)	26 (60.5)	3.39	0.065
Lymphadenopathy	5 (18.5)	0 (0)	8.57	<b>0.003</b>

\*Chi-square test. MOC: mucinous ovarian carcinoma; MBOT: mucinous borderline ovarian tumor. Statistically significant values are indicated in bold.

**Table 2.** Results of logistic regression analysis.

	B	SE	Exp (B)	p-value	95%CI
Constant	2.397	1.066	10.985	0.025	-
Abnormal ascites	0.121	1.139	1.129	0.864	0.121–10.529
Peritoneal carcinomatosis	-21.194	11405.94	0.000	0.999	0.000
Mural nodule (>5 mm)	-0.335	0.850	0.715	0.694	0.135–3.787
Honeycomb sign	3.306	1.208	27.286	<b>0.006</b>	2.559–290.970
Septa	-4.335	1.579	0.013	<b>0.006</b>	0.001–0.289
Lymphadenopathy	-17.253	14704.46	0.000	0.999	0.000

Dependent variable encoding (0: MOC; 1: MBOT). Nagelkerke R<sup>2</sup>: 0.661. MOC: mucinous ovarian carcinoma; MBOT: mucinous borderline ovarian tumor. The bolded values show that the p value is statistically significant. The honeycomb sign and the septa are predictive features for the mucinous borderline tumors.

## DISCUSSION

As observed within the spectrum of mucinous neoplasms, MOCs can develop from MBOTs after going through multiple stages of carcinogenesis<sup>12–14</sup>. Histopathologically, invasive carcinoma and areas showing borderline features can be simultaneously observed in the same mass. Intraoperative consultation/frozen results may not be definitive in terms of diagnosis due to the large size of mucinous tumors and heterogeneity in the epithelial ovarian tumors. Consequently, understaging has been observed in approximately one-third of mucinous ovarian tumor cases<sup>15,16</sup>. Therefore, it is important to distinguish between MBOT and MOC preoperatively to determine the surgical approach.

In our study, the presence of ascites, MN>5 mm, peritoneal involvement, thick septa>5 mm, and the presence of LAP were observed to be significantly higher in MOC cases than in

MBOT cases (Figure 1). Honeycomb appearance was found to be more significant in the MBOT group. The aim was to identify the variables that have a direct and independent effect on determining the groups when the variables that differ between two groups are included in the logistic regression analysis. The results showed that “honeycomb appearance” and “thick septa” determine the difference between groups independently and directly (Table 2). Beta value was positive in the presence of honeycomb sign and was negative in the presence of thick septa. This finding was interpreted as the “honeycomb sign” directly predicts the presence of MBOT and is considered to have diagnostic significance, while “thick septa” is found to predict the MOC group directly (Figure 2).

In previous studies<sup>17,18</sup>, MBOT is shown to be encountered in a wide age group (13–88 years) and the mean age of the patients was 40–49 years, while the mean age in the MOC

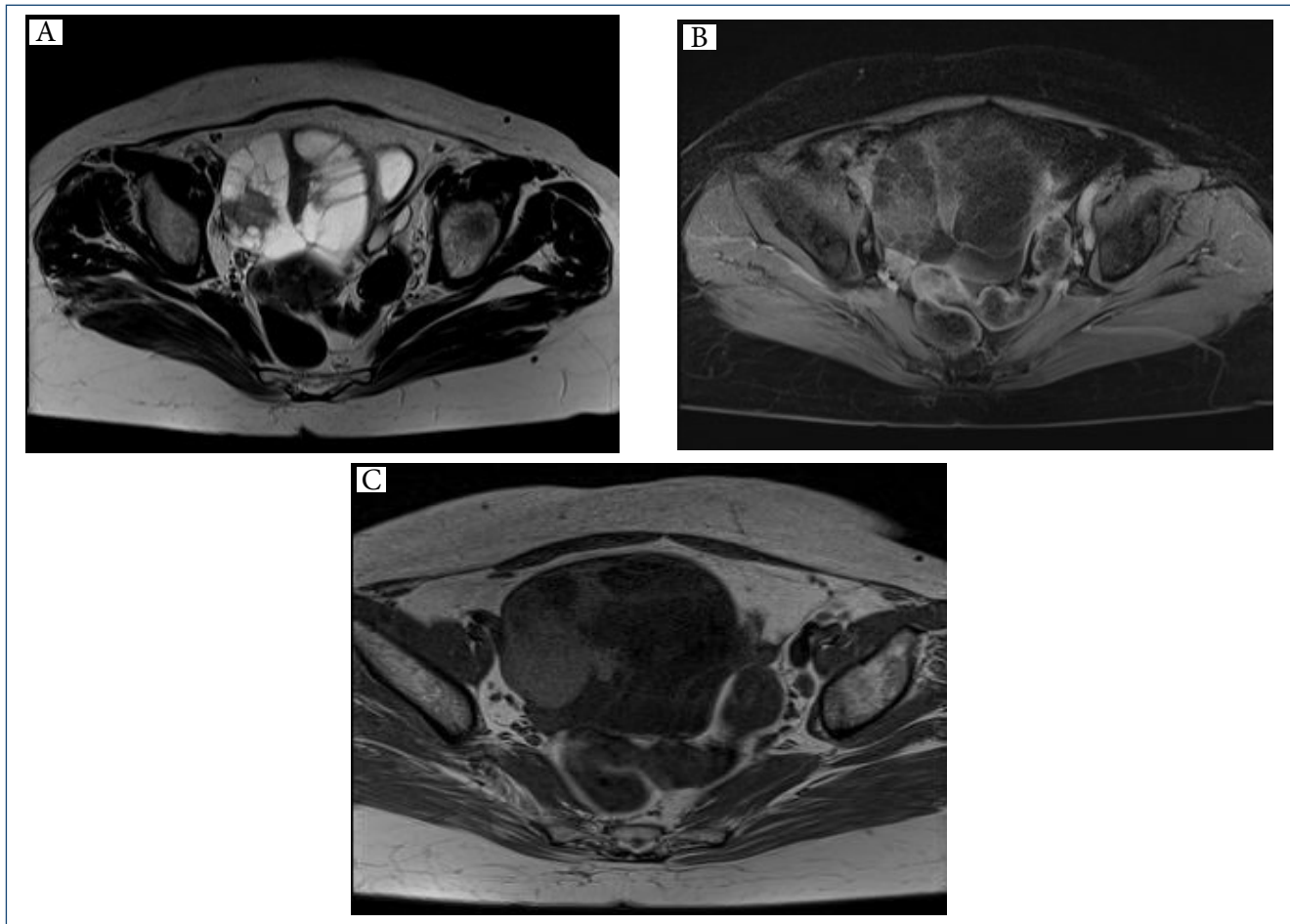


**Figure 1.** A 42-year-old woman with mucinous borderline tumor. (A) Axial T2-weighted image shows multilocular cystic tumor with stained glass appearance (arrow) and honeycomb sign (arrowhead). (B) T1-weighted image shows multilocular cystic tumor with stained glass appearance. (C) Contrast-enhanced T1-weighted image shows enhanced multiple thin septa.

group was 53 years. Consistently, the MOC group has been observed to consist of older patients compared to the MBOT group in our study as well. Our results revealed no significant difference between MBOT and MOC cases in terms of tumor size, though Kaga et al.<sup>19</sup> reported that tumor size in MOC cases was larger than in MBOT cases. In our experience, evaluating the tumor size alone may not be sufficient to distinguish carcinomas from borderline lesions, as all lesions within the spectrum of mucinous neoplasms (including cystadenomas) often present as large masses.

A solid component adhering to the septa or cyst wall was described as a mural nodule and evaluated accordingly. The presence of solid components may suggest malignancy as per the generally accepted view. In our study, the presence of MN was observed significantly more in the MOC group. However, a solid component was also detected in a substantial number of MBOT cases. Yang et al.<sup>20</sup> observed that the maximum size of the solid component is significantly larger

in the MOC group when compared to the MBOT group. Upon reviewing the literature, we have come across a report of an MBOT case with a large solid component, published by Kozawa et al.<sup>21</sup>, pointing out that evaluating the solid component alone can make the differential diagnosis process harder. Hence, the necessity of evaluating all parameters and the importance of synthesizing all of the findings to make differential diagnoses have arisen.

Among other findings, the presence of thick septa and ascites has been observed more in MOC cases than MBOT cases in our study. In Yang et al.'s<sup>20</sup> study, the presence of ascites was observed to be significantly more frequent in carcinoma cases. Similar statistically significant results have been noted in our study, as nine of our MOC patients and five of our MBOT patients had ascites. However, in our present sample, peritoneal washing cytology specimens of both groups were hypocellular and were negative for malignancy. The large size of mucinous neoplasms may create pressure, resulting in

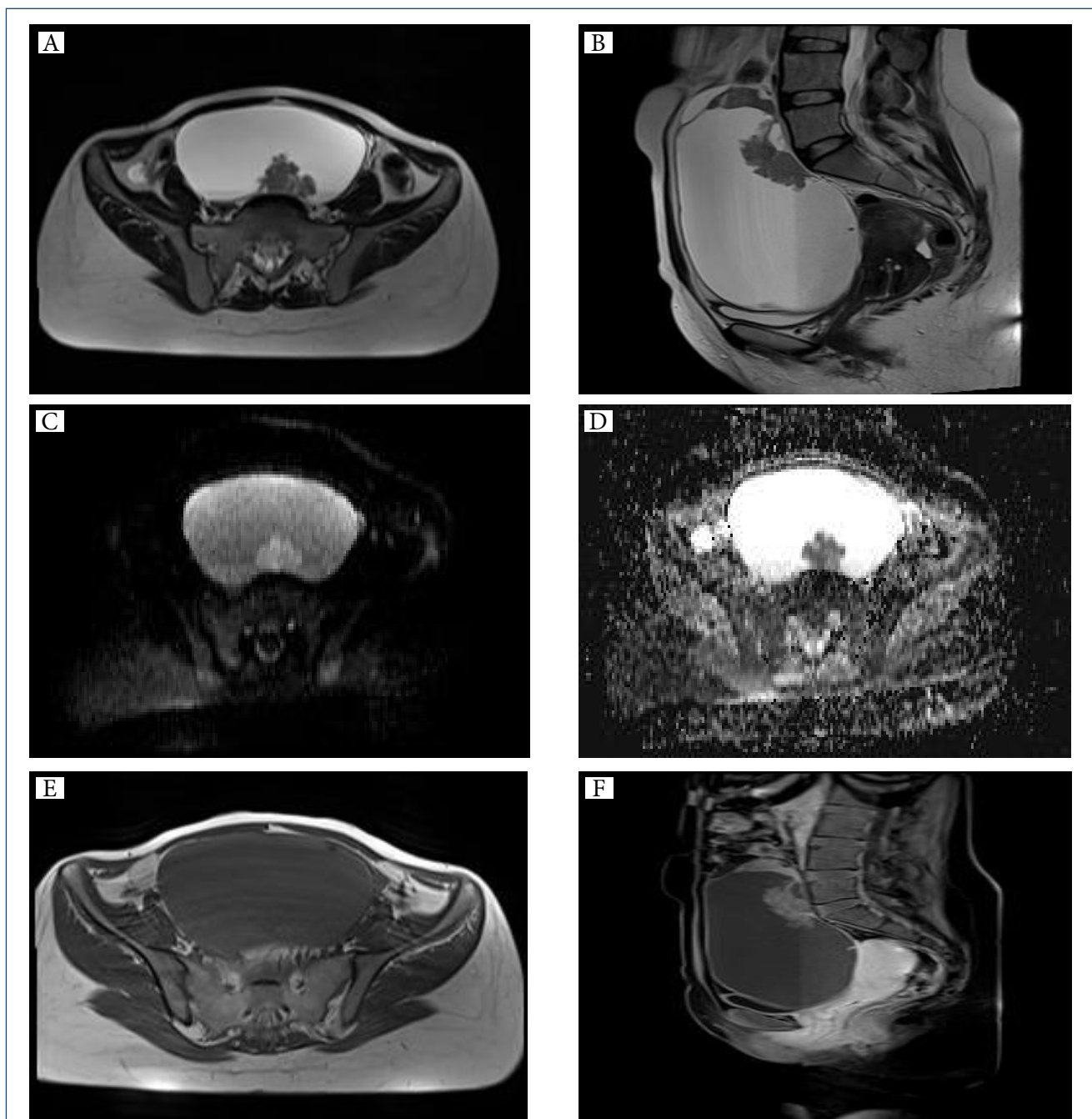


**Figure 2.** A 53-year-old woman with mucinous carcinoma. **(A and B)** Axial and sagittal T2-weighted image shows a gross multilocular cystic tumor with a mildly hyperintense mural nodule larger than 5 mm (arrow). **(C)** Diffusion-weighted image shows a hyperintense mural nodule (arrow). **(D)** Apparent diffusion coefficient (ADC) map shows a low ADC value. **(E)** T1-weighted image shows a hypointense mural nodule (arrow). **(F)** Contrast-enhanced T1-weighted image shows a moderately enhanced mural nodule (arrow).

congestion findings on the peritoneum and possible development of ascites.

Due to the proliferation rate of malignant tumor cells, MBOTs appear as masses with heterogeneous internal structures with thicker walls and septum, harboring more solid components (Figure 1).

There are some limitations to our study. First of all, our study is retrospective, and the number of patients with carcinoma is low. It was difficult to detect the thickest septa during the measurement of “thick septa” because mucinous neoplasms are known to have a multiseptal appearance. As a result, the contribution of “apparent diffusion coefficient (ADC)” values

to the diagnosis could not be examined either. We think that ADC measurement from the level of the septa or millimeter-sized mural nodule may be misleading, especially at these small sizes.

## CONCLUSION

The MRI findings of MOCs and MBOTs are similar. MOCs tend to have larger tumor sizes and larger mural nodules, and the development of ascites is observed to be more frequent. “Honeycomb sign” can be used as a specific MRI finding for MBOT cases.

## INSTITUTIONAL REVIEW BOARD STATEMENT

The study was conducted according to the guidelines of the Declaration of Helsinki and approved by the Ethics Committee of our hospital.

## REFERENCES

1. Prat J, D'Angelo E, Espinosa I. Ovarian carcinomas: at least five different diseases with distinct histological features and molecular genetics. *Human Pathol.* 2018;80:11-27. <https://doi.org/10.1016/j.humpath.2018.06.018>
2. Taylor HC. Malignant and semimalignant tumors of the ovary. *Surg Gynecol Obstet.* 1929;48:204-30.
3. Prat J, Nicolis DM. Serous borderline tumors of the ovary: a long-term follow-up study of 137 cases, including 18 with a micropapillary pattern and 20 with microinvasion. *Am J Surg Pathol.* 2002;26(9):1111-28. <https://doi.org/10.1097/00000478-200209000-00002>
4. Riepel MA, Ronnett BM, Kurman RJ. Evaluation of diagnostic criteria and behavior of ovarian intestinal-type mucinous tumors: atypical proliferative (borderline) tumors and intraepithelial, microinvasive, invasive, and metastatic carcinomas. *Am J Surg Pathol.* 1999;23(6):617-35. <https://doi.org/10.1097/00000478-199906000-00001>
5. Wagner BJ, Buck JL, Seidman JD, McCabe KM. From the archives of the AFIP. Ovarian epithelial neoplasms: radiologic-pathologic correlation. *Radiographics.* 1994;14(6):1351-74. <https://doi.org/10.1148/radiographics.14.6.7855346>
6. Tanaka Y, Nishida M, Kurosaki Y, Itai Y, Tsunoda H, Kubo T. Differential diagnosis of gynaecological “stained glass” tumours on MRI. *Br J Radiol.* 1999;72(856):414-20. <https://doi.org/10.1259/bjr.72.856.10474509>
7. Outwater EK, Huang AB, Dunton CJ, Talerma A, Capuzzi DM. Papillary projections in ovarian neoplasms: appearance on MRI. *J Magn Reson Imaging.* 1997;7(4):689-95. <https://doi.org/10.1002/jmri.1880070414>
8. Mitchell DG. Magnetic resonance imaging of the adnexa. *Semin Ultrasound CT MR.* 1988;9(2):143-57.
9. Mitchell DG, Mintz MC, Spritzer CE, Gussman D, Arger PH, Coleman BG, et al. Adnexal masses: MR imaging observations at 1.5 T, with US and CT correlation. *Radiology.* 1987;162(2):319-24. <https://doi.org/10.1148/radiology.162.2.3541026>

## DATA AVAILABILITY STATEMENT

There are no publicly stored datasets associated with this paper. Data are available upon request, from the corresponding author.

## INFORMED CONSENT STATEMENT

Informed consent was not obtained because the study was in a retrospective design.

## AUTHORS' CONTRIBUTIONS

**EH:** Conceptualization, Data curation, Formal Analysis, Funding acquisition, Investigation, Methodology, Project administration, Resources, Visualization, Writing—original draft, Writing – review & editing. **GG:** Data curation, Resources. **BGO:** Writing—review & editing. **MS:** Conceptualization, Data curation, Resources, Supervision.

10. Stevens S, Hricak H, Stern J. Ovarian lesions: detection and characterization with gadolinium-enhanced MR imaging at 1.5 T. *Radiology.* 1991;181(2):481-8. <https://doi.org/10.1148/radiology.181.2.1924792>
11. Armstrong DK, Alvarez RD, Bakkum-Gamez JN, Barroilhet L, Behbakht K, Berchuck A, et al. NCCN guidelines insights: ovarian cancer, version 1.2019: featured updates to the NCCN guidelines. *J Natl Comprehensive Cancer Network.* 2019;17(8):896-909. <https://doi.org/10.6004/jnccn.2019.0039>
12. Mackenzie R, Kommoss S, Winterhoff BJ, Kipp BR, Garcia JJ, Voss J, et al. Targeted deep sequencing of mucinous ovarian tumors reveals multiple overlapping RAS-pathway activating mutations in borderline and cancerous neoplasms. *BMC Cancer.* 2015;15(1):415. <https://doi.org/10.1186/s12885-015-1421-8>
13. Lee Y-J, Lee M-Y, Ruan A, Chen C-K, Liu H-P, Wang C-J, et al. Multipoint Kras oncogene mutations potentially indicate mucinous carcinoma on the entire spectrum of mucinous ovarian neoplasms. *Oncotarget.* 2016;7(50):82097. <https://doi.org/10.18632/oncotarget.13449>
14. Marko J, Marko KI, Pachigolla SL, Crothers BA, Mattu R, Wolfman DJ. Mucinous neoplasms of the ovary: radiologic-pathologic correlation. *Radiographics.* 2019;39(4):982-97. <https://doi.org/10.1148/rg.2019180221>
15. Capozzi VA, Sozzi G, Uccella S, Ceni V, Cianciolo A, Gambino G, et al. Novel preoperative predictive score to evaluate lymphovascular space involvement in endometrial cancer: an aid to the sentinel lymph node algorithm. *Int J Gynecol Cancer.* 2020;30(6):806-812. <https://doi.org/10.1136/ijgc-2019-001016>
16. Morton R, Anderson L, Carter J, Pather S, Saidi SA. Intraoperative frozen section of ovarian tumors: a 6-year review of performance and potential pitfalls in an Australian Tertiary Referral Center. *Int J Gynecol Cancer.* 2017;27(1):17-21. <https://doi.org/10.1097/IGC.0000000000000851>
17. Young R. WHO classification of tumours of female reproductive organs. In: Kurman RJ, Carcangiu ML, Herrington CS, Young RH, editors. *Monodermal teratomas and somatic-type tumours arising from a dermoid cyst.* Geneva: WHO; 2014. p. 63-6.

18. Morice P, Gouy S, Leary A. Mucinous ovarian carcinoma. *N Engl J Med.* 2019;380(13):1256-66. <https://doi.org/10.1056/NEJMra1813254>
19. Kaga T, Kato H, Hatano Y, Kawaguchi M, Furui T, Morishige K-I, et al. Can MRI features differentiate ovarian mucinous carcinoma from mucinous borderline tumor? *Eur J Radiol.* 2020;132:109281. <https://doi.org/10.1016/j.ejrad.2020.109281>
20. Yang X, Li X, Ma F, Li H, Zhao S, Li Y, et al. MRI characteristics for differentiating mucinous borderline ovarian tumours from mucinous ovarian cancers. *Clin Radiol.* 2022;77(2):142-7. <https://doi.org/10.1016/j.crad.2021.10.022>
21. Kozawa E, Inoue K, Yano M, Yasuda M, Hasegawa K, Tanaka J, et al. An unusual ovarian mucinous borderline tumor with a large solid component. *Case Rep Radiol.* 2019;2019:1402736. <https://doi.org/10.1155/2019/1402736>

